ELSEVIER

J. Non-Newtonian Fluid Mech. 127 (2005) 143–155

Journal of Non-Newtonian Fluid Mechanics

www.elsevier.com/locate/jnnfm

Observations of asymmetrical flow behaviour in transitional pipe flow of yield-stress and other shear-thinning liquids

M.P. Escudier [a,*], R.J. Poole [a], F. Presti [a], C. Dales [a], C. Nouar [b], C. Desaubry [b], L. Graham [c], L. Pullum [c]

[a] *University of Liverpool, Department of Engineering, Mechanical Engineering, Brownlow Hill, Liverpool L69 3GH, UK*
[b] *LEMTA-Laboratoire d'Energetique et de Mecanique Theorique et Appliquee UMR 7563, 2, Avenue de la Foret de Haye, BP 160, 54 504 Vandoeuvre-les-Nancy Cedex, France*
[c] *Energy and Thermofluids Engineering, CSIRO MIT, Graham Road, Highett, Vic. 3190, Australia*

Received 20 December 2004; received in revised form 11 February 2005; accepted 12 February 2005

Abstract

The purpose of this brief paper is to report mean velocity profile data for fully developed pipe flow of a wide range of shear-thinning liquids together with two Newtonian control liquids. Although most of the data reported are for the laminar–turbulent transition regime, data are also included for laminar and turbulent flow. The experimental data were obtained in unrelated research programmes in UK, France and Australia, all using laser Doppler anemometry (LDA) as the measurement technique. In the majority of cases, axisymmetric flow is observed for the laminar and turbulent flow conditions, although asymmetry due to the Earth's rotation is evident for the laminar flow of a Newtonian fluid of low viscosity (i.e. low Ekman number). The key point, however, is that for certain fluids, both yield-stress and viscoelastic (all fluids in this study are shear-thinning), asymmetry to varying degrees is apparent at all stages of transition from laminar to turbulent flow, i.e. from the first indications to almost fully developed turbulence. The fact that symmetrical velocity profiles are obtained for both laminar and turbulent flow of all the non-Newtonian fluids in all three laboratories leads to the conclusion that the asymmetry must be a consequence of a fluid-dynamic mechanism, as yet not identified, rather than imperfections in the flow facilities.

Keywords: Yield-stress; Shear-thinning; Pipe flow; Asymmetry

1. Introduction

Consistent with the concept of fully developed flow in a circular pipe is the expectation that the radial distributions of mean velocity will be axisymmetric irrespective of whether the flow is laminar, turbulent or transitional. In fact, as [4] have shown, under certain circumstances significant departures from axisymmetry in fully developed laminar pipe flow of a Newtonian fluid can arise as a consequence of the influence of the Coriolis acceleration due to the Earth's rotation. An experimental study of laminar–turbulent transition in fully developed laminar pipe flow [5] showed that if such a flow is subjected to a relatively high amplitude, asymmetrical disturbance upstream, then the mean velocity profiles for the downstream flow exhibited an asymmetric distortion. Apart from these rather special situations, so far as Newtonian fluids are concerned we are unaware of any evidence to suggest that the expectation of mean-flow axisymmetry in fully developed pipe flow is unfounded for any of the three flow regimes. As a consequence of the interest in drag reduction, a number of papers have been published concerned primarily with the fully developed turbulent pipe flow of very low concentrations of high molecular weight polymers [1,2,9,10,16–18]. The velocity profile data for these turbulent flows appear to be axisymmetric as do data for the flow of non-Newtonian liquids (for the most part higher concentrations of polymers) [11,12,14]. The same can be said for the limited data for fully developed laminar flow, which these authors included with that for their turbulent flows. For

* Corresponding author. Tel.: +44 15179 44848; fax: +44 15179 44805.
E-mail address: escudier@liv.ac.uk (M.P. Escudier).

0377-0257/$ – see front matter © 2005 Elsevier B.V. All rights reserved.
doi:10.1016/j.jnnfm.2005.02.006

transitional flow the only published data we are aware of is for Laponite [6], a synthetic clay, which is shear-thinning with a yield-stress and is also thixotropic. This flow was found to be strongly asymmetric and it was originally thought that minor imperfections in the flow geometry were the cause, notwithstanding the axisymmetric appearance of velocity profiles for Laponite flows under laminar and turbulent flow conditions.

The purpose of this brief paper is to report mean velocity profile data for the flow of a wide range of shear-thinning liquids primarily in the laminar–turbulent transition regime. The data were obtained in three unrelated research programmes in UK, France and Australia, all using laser Doppler anemometry (LDA) as the measurement technique. These data include measurements obtained in the 100 mm i.d. pipe flow facility in Liverpool additional to those reported by Escudier and Presti [6], all of which show departures from axisymmetry in the transition regime. Other data revealing a lack of axisymmetry are reported for experiments carried out in a much smaller pipe run (30 mm i.d.) in LEMTA, Nancy, and in a larger facility (105 mm i.d.) at CSIRO, Melbourne. Because the data were collected quite independently and at different points in time, inevitably there are differences in methodology and completeness. None of these differences is substantial so far as the conclusions are concerned.

2. Experimental facilities

Full details of the flow facility and instrumentation at the University of Liverpool have been given by Escudier and Presti [6] and so only the briefest of descriptions is given here. The measurements were obtained using a Dantec Fibre Flow LDA system with a measuring volume 0.2 mm in length and 20 μm in diameter (in water) in a glass pipe of internal diameter 100 ± 0.4 mm at a location 12 m (120 diameters) from the pipe inlet. Rheological data for the liquids used were obtained using a Bohlin VOR controlled stress rheometer.

The LEMTA, Nancy, measurements were carried out in a plexiglass tube 30 mm i.d. and 4.5 m from the inlet (i.e. 150 diameters). Details of this pipe flow facility are given by Peixinho et al. [13]. These velocity measurements were carried out using a Dantec FlowLite LDA system with a measuring volume 0.65 mm in length and 77 μm in diameter for the main body of the flow and 0.17 mm length and 39 μm diameter for the near-wall region. The rheological measurements were performed using a TA Instruments AR 2000 controlled stress rheometer.

The measurements carried out at the CSIRO, Melbourne, laboratory were performed in a PVC pipe 105 mm in diameter equipped with a plexiglass section for optical access situated 20 m (190 diameters) downstream of a bend. Details of this pipe flow facility are given by Graham and Pullum [8]. The velocity measurements were made using a two-colour TSI LDV system and the rheological parameters of the liquids used were obtained using a Bohlin CVO50 controlled stress rheometer.

For the LDA systems used in each of the three laboratories, the total uncertainty in the mean velocity values is estimated to be typically 3–4% (see, e.g. [15]). Error bars representing this low level of uncertainty would be smaller than the symbols used in Figs. 3(a)–13(a) and so have not been included. It is clear that the measurement uncertainty cannot account for the observed asymmetry.

3. Rheological data

The working liquids used in Liverpool were aqueous solutions of 1.5 wt% Laponite (which we abbreviate as LAP LIV) [grade RD supplied by Laporte Industries Ltd.], 0.1% Carbopol EZ1 (CARB LIV) [Carbopol EZ1 supplied by Sursachem Ltd.], 0.25% sodium carboxymethylcellulose (CMC LIV) [supplied by BDH Ltd.], 0.2% xanthan gum (XG LIV) [Keltrol TF supplied by Kelco], a blend of 0.09% CMC and 0.09% XG (CMC/XG LIV) [same suppliers as unblended polymers] and 0.125 and 0.2% polyacrylamide (PAA LIV) [Separan AP 273 E supplied by Floerger]. The shear viscosity data for Laponite and high (>0.1%) concentrations of Carbopol are found to be best characterised by the Herschel–Bulkley model:

$$\tau = \tau_Y + K(\dot{\gamma})^n, \quad \tau > \tau_Y \tag{1}$$

while all other liquids are well represented by the Carreau–Yasuda model:

$$\mu_{CY} = \mu_\infty + \frac{\mu_0 - \mu_\infty}{(1 + (\lambda_{CY}\dot{\gamma})^a)^{n/a}} \tag{2}$$

In equation (1), τ is the shear stress, τ_Y the "yield-stress", K a consistency parameter, n the power-law index and $\dot{\gamma}$ is the shear rate. The additional quantities which appear in equation (2) are μ_{CY}, the apparent viscosity according to the Carreau–Yasuda model, μ_∞ the viscosity at infinite shear rate, μ_0 the viscosity at zero shear rate, λ_{CY} a time constant and a is a parameter introduced by Yasuda et al. [20]. The shear viscosity data are shown in Figs. 1 and 2 together with curves representing the two models, as appropriate. The model parameters for the solutions, which are best represented by the Carreau–Yasuda model, are listed in Table 1 and those well fitted by the Herschel–Bulkley in Table 2.

The working liquid for the LEMTA laboratory was an aqueous solution of 0.2% Carbopol 940 (CARB LEMTA) supplied by Noveon Inc.

The working liquids for the CSIRO, Melbourne, measurements were aqueous solutions of 0.08% Ultrez 10, a variety of Carbopol supplied by BF Goodrich (ULTREZ CSIRO) and 0.6% sodium carboxymethylcellulose (7HF Aqualon) supplied by A.C. Hatrick (CMC CSIRO).

It is well known that many of the working liquids used in the various experiments discussed in this paper are to varying degrees viscoelastic and that this characteristic strongly

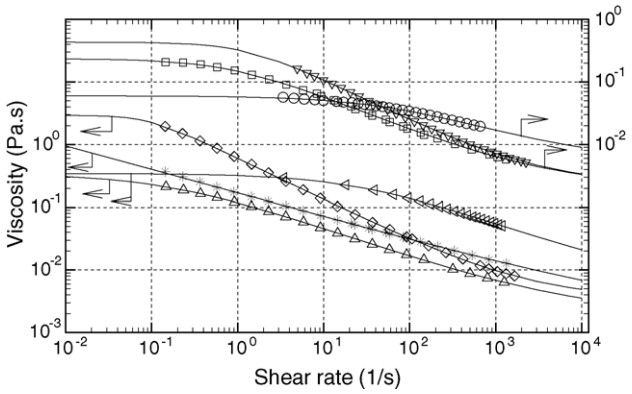

Fig. 1. Viscometric data for various polymer solutions (including Carreau–Yasuda fit), (△) 0.09% CMC/0.09% XG LIV, (◯) 0.25% CMC LIV, (□) 0.125% PAA LIV, (◊) 0.2% PAA LIV, (▽) 0.2% XG LIV, (✳) 0.1% CARB LIV, (◁) 0.6% CMC CSIRO.

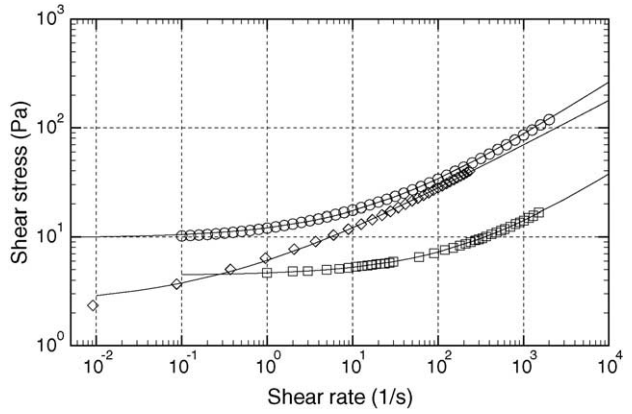

Fig. 2. Flow curves for yield-stress type behaviour (including Herschel–Bulkely fits), (□) 1.5% LAP LIV, (◊) 0.08% ULTREZ CSIRO, (◯) 0.2% CARB LEMTA.

Table 1
Carreau–Yasuda model parameters for polymer solutions

Fluid	μ_0 (Pa s)	$\mu_\infty \times 10^{-3}$ (Pa s)	λ_{CY} (s)	n	a
0.1% CARB LIV	5.92	1.65	13000	0.376	7.4
0.25% CMC LIV	0.0599	5.51	0.0125	0.562	0.669
0.09% CMC/0.09% XG LIV	0.342	1.93	6.26	0.484	0.656
0.125% PAA LIV	0.235	2.19	1.12	0.572	0.910
0.2% PAA LIV	2.94	3.55	11.1	0.660	2.01
0.2% XG LIV	0.431	2.35	0.778	0.673	1.29
0.6% CMC CSIRO	0.344	5.45	0.0378	0.514	0.686

Table 2
Herschel–Bulkley model parameters for yield-stress fluids

Fluid	τ_Y (Pa)	K (Pa s^n)	n
1.5% LAP LIV	4.42	0.242	0.534
0.2% CARB LEMTA	9.8	2.31	0.51
0.08% ULTREZ CSIRO	2.39	3.64	0.423

influences the turbulent flow structure and delays transition. Unfortunately, the set of viscoelastic data (i.e. the storage modulus G', the loss modulus G'', the first normal-stress difference N_1 and the extensional viscosity) is far less complete than is the case for the viscometric data and so no viscoelastic data are included here, although it is worth noting that attempts to measure viscoelastic behaviour for the CSIRO Ultrez and Carbopol solutions using a Rheometrics ARES rheometer (fitted with 50 mm parallel plates) failed to resolve any significant values for N_1 and the second normal-stress difference N_2. Such further data as are available can be found in [7,13].

4. Experimental data

Each set of velocity profiles shown in Figs. 3(a)–13(a) covers a range of Reynolds numbers which span the three flow regimes. The definition adopted for the Reynolds number is

$$Re = \frac{\rho U_B D}{\mu_W} \tag{3}$$

where ρ is the liquid density (essentially that of water for the low concentrations under consideration here), U_B the bulk velocity (i.e. flow rate/pipe cross-sectional area) and D is the pipe diameter. The viscosity μ_W for the non-Newtonian liquids, all of which to various degrees are shear-thinning, was determined from either the Herschel–Bulkley model fit (for LAP and 0.2% CAR) or the Carreau–Yasuda model fit (for 0.1% CAR, CMC, XG, CMC/XG and PAA) at a shear rate taken as the velocity gradient at the pipe wall. Also included with each set of velocity profiles are reference curves corresponding to an average of the velocity data on either side of the centreline. Where the experimental data follow a smooth curve, as in the laminar flow regime, the corresponding reference curves are also smooth. In the transitional regime, where the data show much more variability, the reference curves are more jagged in appearance but still symmetrical (by construction). The sequence of figures showing the velocity profiles starts with the data for water and glycerol (i.e. Newtonian fluids) and is followed by data for the non-Newtonian liquids, which reveal a progressively decreasing degree of asymmetry. The velocity profiles for each fluid are presented in order of increasing Reynolds number offset from bottom to top by an amount indicated by the shifted origins depicted by '0' along the ordinate of each figure. The actual velocity scale is shown in each case for the profile at the highest Reynolds number. Below each set of velocity profiles is the variation with Reynolds number of the near-wall ($r/R = 0.8$, where r is the radial location within the pipe and R is the pipe radius) axial-velocity fluctuation level u' (rms), which [6] was found to be an excellent indicator of the flow regime. The highlighted symbols in the u' (Re) plots in part (b) of Figs. 3–13 correspond to the Re values for the velocity profiles in part (a) of each figure. The flow parameters for all flows are listed in Table 3.

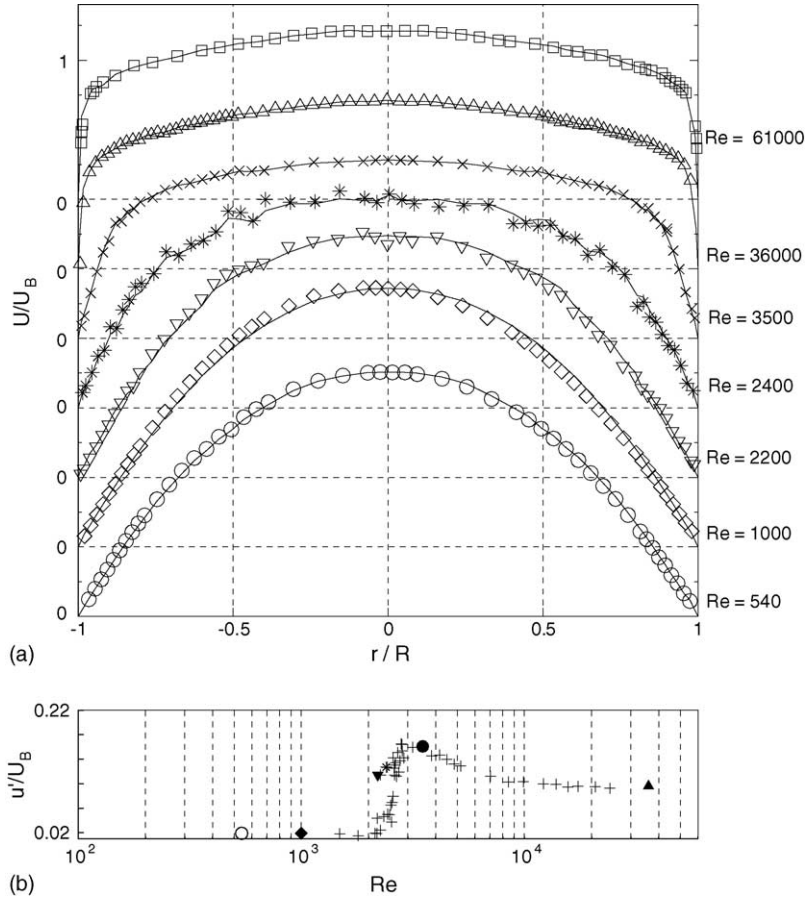

Fig. 3. (a) Mean axial velocity profiles for Newtonian fluids LIV (including average data line) and (b) axial fluctuation level at $r/R = 0.8$ to indicate transition.

The slight asymmetry in the velocity profiles for glycerol (Fig. 3(a)) at $Re = 540$ and 1000 is consistent with the observations of Draad and Nieuwstadt [4] and their argument that asymmetry in fully developed laminar flow is due to the Earth's rotation and is governed by an Ekman number defined as

$$Ek = \frac{\mu_W}{2\Omega\rho D^2 \sin\alpha} \tag{4}$$

where Ω is angular velocity of the Earth (i.e. $7.272 \times 10^{-5}\,s^{-1}$) and α is the angle between the pipe axis and the rotation axis of the Earth. In fully developed laminar flow through a straight circular pipe, the streamlines are parallel, viscous forces are balanced by pressure forces, the fluid inertia is unchanging and so plays no role in the fluid-dynamic. The influence of the Coriolis acceleration due to the combined effects of the Earth's rotation and the parallel flow is to generate a component of acceleration transverse to the pipe axis which leads to a distortion of the velocity profile. The Liverpool pipe run is oriented along a west–east axis and the latitude for Liverpool is 52°N, which in this case also equals the angle α. The corresponding Ekman number for the glycerol flow is 5, which is practically the same as the value of 5.2 for the experiments of Draad and Nieuwstadt. The lower the value of *Ek*, the more important rotational effects become compared with viscous forces. So far as the present paper is concerned the Ekman number is certainly relevant for the fully developed laminar flows and in Table 3 the values of the Ekman number are listed only for this flow condition.

Other influences, which could lead to asymmetry, include buoyancy arising from ambient temperature gradients and curvature of the pipe axis. Dean [3] was the first to investigate systematically the effect of curvature. His work led to the conclusion that the parameter (now termed the Dean number, *De*), which determines the strength of secondary flows due to curvature is

$$De = Re\left(\frac{D}{2R_A}\right)^{1/2} \tag{5}$$

where R_A is the radius of curvature of the pipe axis. Curvature becomes important if $De > 40$ which, for the Liverpool pipe flow facility, requires $R_A < 125$ m for $Re = 2000$ or a 100 mm departure from straightness over a length of 10 m, which is at least two orders of magnitude greater than is the case. Buoyancy effects are unlikely to be significant because they require a sustained uniform temperature gradient in the vicinity of the pipe run, whereas in practice the ambient temperature is more likely to fluctuate with time and location.

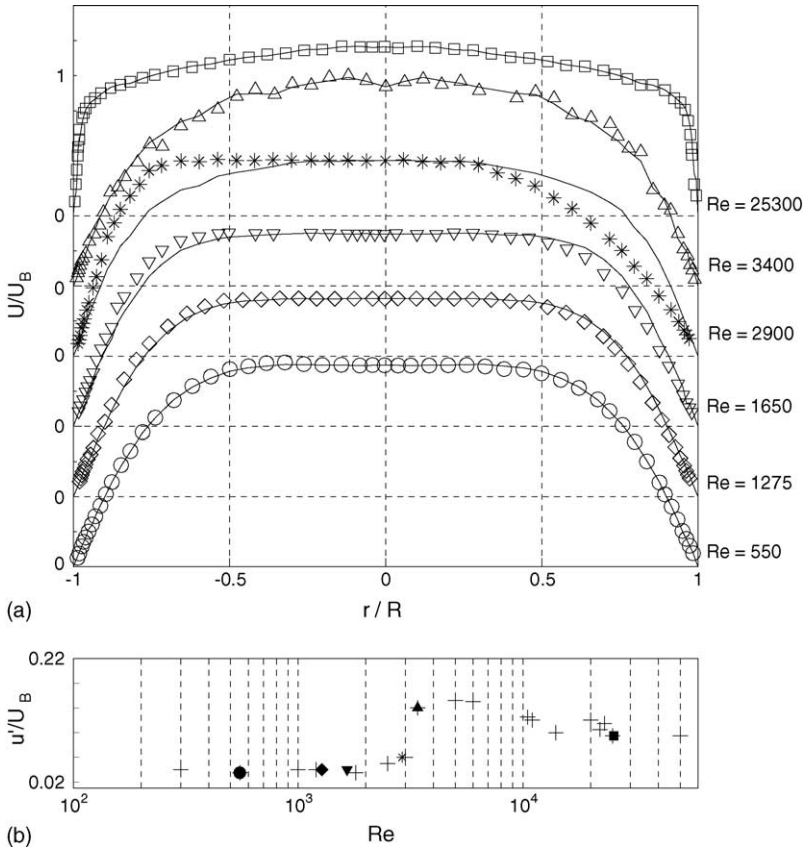

Fig. 4. (a) Mean axial velocity profiles for 1.5% LAP LIV (including average data line) and (b) axial fluctuation level at $r/R = 0.8$ to indicate transition.

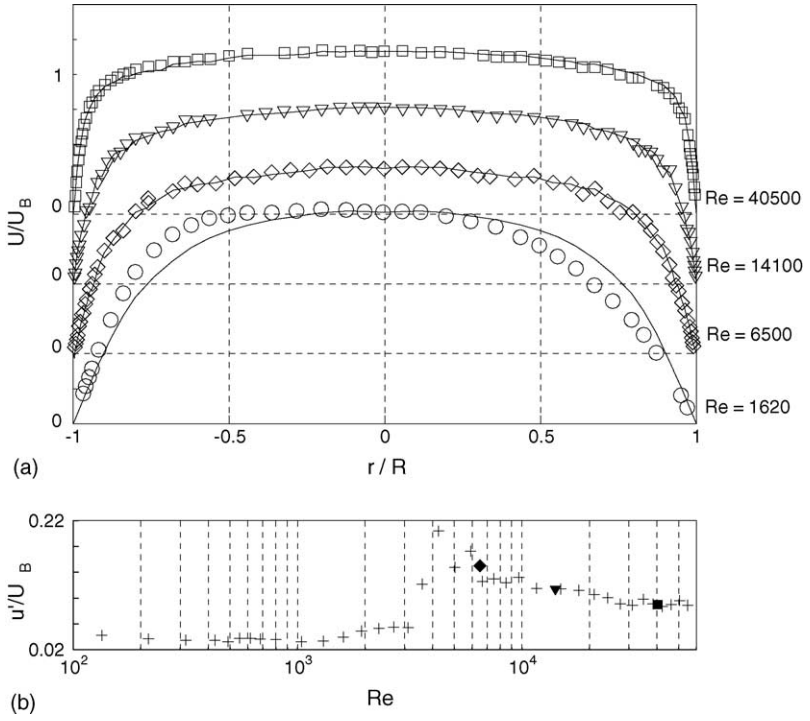

Fig. 5. (a) Mean axial velocity profiles for 0.2% XG LIV (including average data line) and (b) axial fluctuation level at $r/R = 0.8$ to indicate transition.

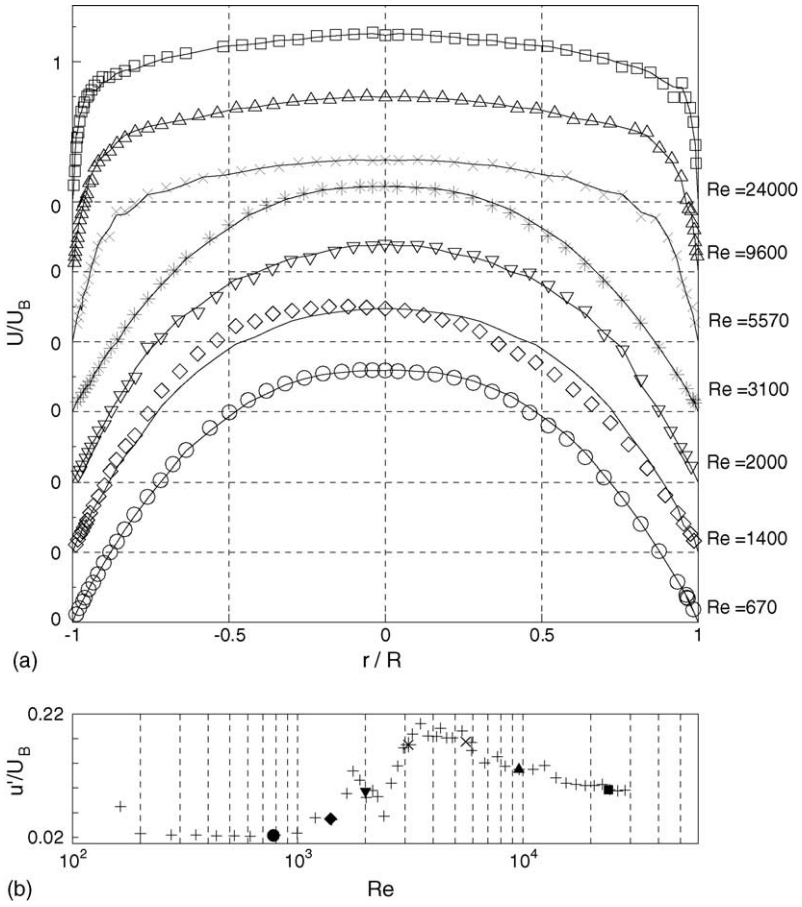

Fig. 6. (a) Mean axial velocity profiles for 0.1% CARB LIV (including average data line) and (b) axial fluctuation level at $r/R = 0.8$ to indicate transition.

The asymmetry persists for the profile at $Re = 2200$ and has almost disappeared for that at $Re = 2400$. As is well known (e.g. [19]), transition in fully developed pipe flow for a Newtonian fluid is normally taken to occur between a Reynolds number of about 2000 (the start of laminar instability) and 4000 (by which point the flow is fully turbulent), so both of these profiles correspond to an early stage of the transition process. A very slight asymmetry is still evident for $Re = 2200$ and may result from the Earth's rotation but the degree of asymmetry is so slight that it would almost go unremarked were it not under such close scrutiny. The two turbulent flow profiles for glycerol ($Re = 3500$ and 36,000) and a third for water ($Re = 61{,}000$) are all symmetrical.

The Laponite data in Fig. 4(a) are those originally reported by Escudier and Presti [6]. In contrast to the flow of glycerol, the absence of asymmetry of the laminar flow profile for Laponite at $Re = 550$ can be explained by the fact that this fluid has a much higher kinematic viscosity (9.45×10^{-5} m^2/s), a correspondingly high Ekman number ($Ek = 65$) and the influence of the Coriolis acceleration is considerably reduced. In fact, the Ekman numbers for all the non-Newtonian liquid flows fall in the range 21–65 as shown in Table 3, so in the worst case the Coriolis force amounts to less than 5% of the viscous force compared with 20% for the Newtonian fluid flow. The two subsequent profiles for Laponite ($Re = 1275$ and 1650) are both asymmetric. The profile at $Re = 2900$, which the near-wall fluctuation levels show corresponds to the early stages of transition, is the most asymmetric of any we report here, whereas that for $Re = 3400$ is practically symmetrical but shows far more scatter than all other profiles in this set due to the very high fluctuation levels associated with the final stage of transition. The profile for fully turbulent flow ($Re = 25{,}300$) is clearly symmetrical and almost identical to that for the high Reynolds number flows of glycerol and water.

Xanthan gum is a semi-rigid polymer with a very different structure to Laponite, which is a synthetic clay. Nevertheless, the profile measured in Liverpool shown in Fig. 5(a) for the very start of transition ($Re = 1620$) is again strongly asymmetric in the same sense (i.e. to the left) as the profile for Laponite at the start of transition. The three turbulent flow ($Re = 6500$, 14,100 and 40,500) XG profiles are entirely symmetrical.

In contrast to the data for a higher concentration level (see, Fig. 9(a)), at a concentration level of 0.1%, Carbopol EZ1 (CARB LIV) did not display yield-stress type behaviour and the flow curve for this fluid (Fig. 1) is well represented by the Carreau–Yasuda model fit. The mean axial velocity profiles for this fluid are shown in Fig. 6(a). The laminar

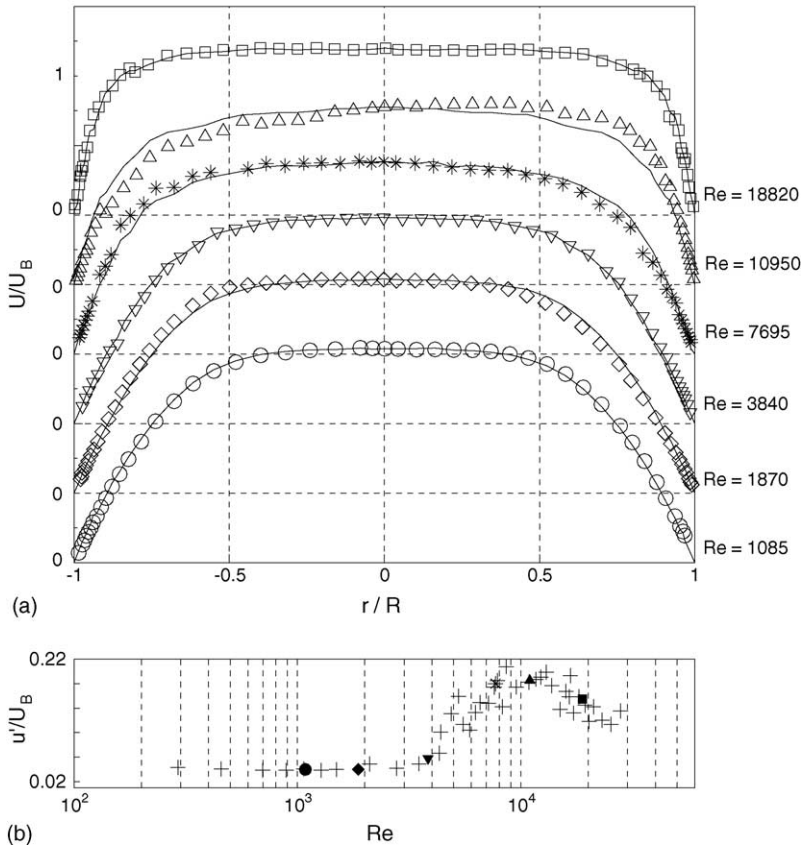

Fig. 7. (a) Mean axial velocity profiles for 0.2% PAA LIV (including average data line) and (b) axial fluctuation level at $r/R = 0.8$ to indicate transition.

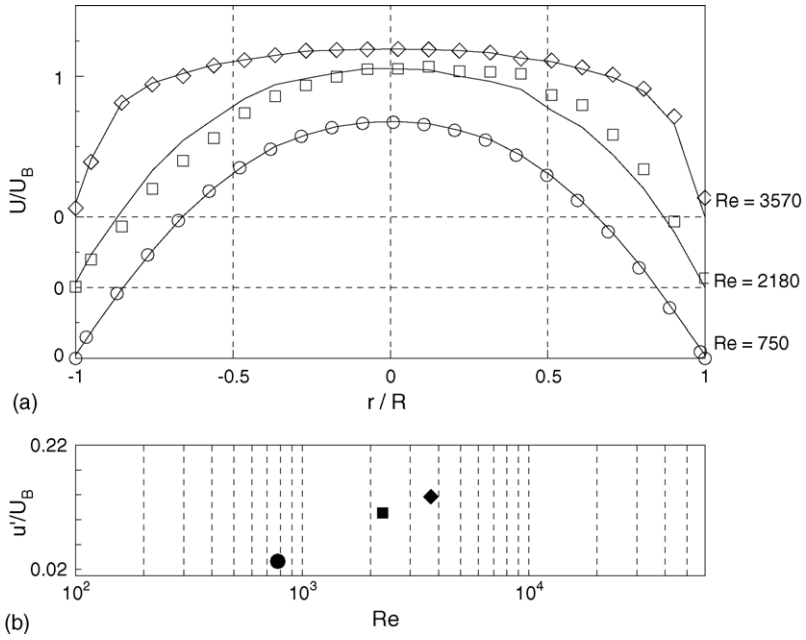

Fig. 8. (a) Mean axial velocity profiles for 0.6% CMC CSIRO (including average data line) and (b) axial fluctuation level at $r/R = 0.8$ to indicate transition.

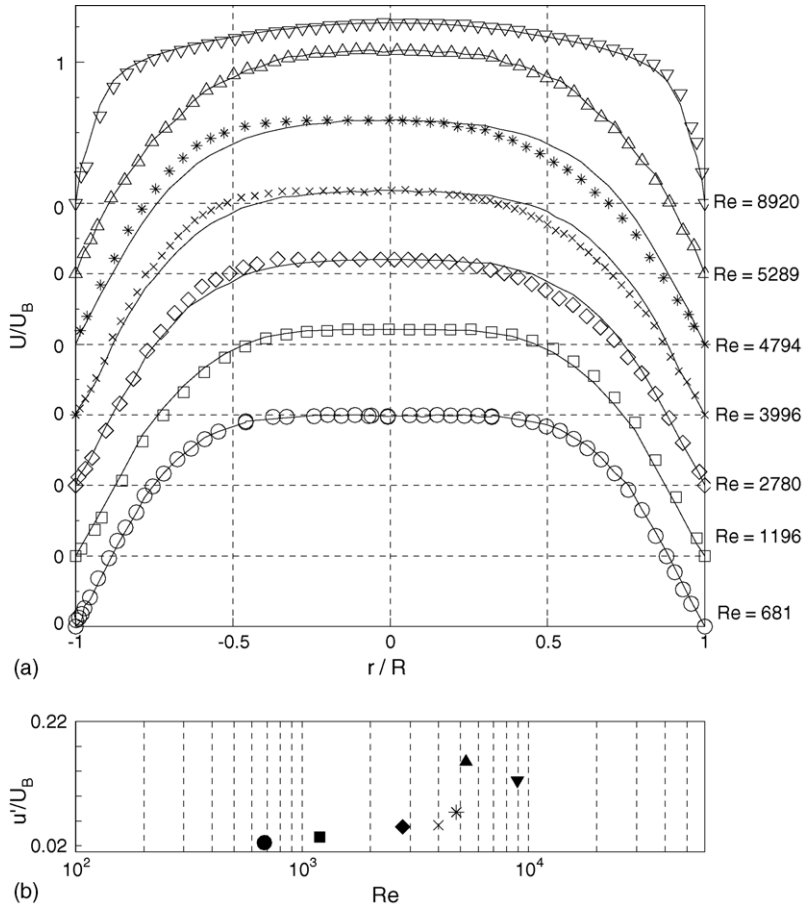

Fig. 9. (a) Mean axial velocity profiles for 0.2% CARB LEMTA (including average data line) and (b) axial fluctuation level at $r/R = 0.8$ to indicate transition.

flow profile at $Re = 670$ is symmetrical but that at $Re = 1400$, which the fluctuation levels suggest is in the early stages of transition, is clearly asymmetrical. Pexinho et al. [13] suggest that transition of yield-stress liquids is a two-stage process and the u' variation in Fig. 6(b) lends credence to this idea. The transitional flow profile at $Re = 2000$ shows a very slight asymmetry to the right in contrast to the asymmetry to the left shown by all other asymmetric profiles discussed so far. The profiles for Carbopol at higher Reynolds numbers, both for transitional ($Re = 3100$) and turbulent flow ($Re = 5570$, 9600 and 24,000) are again all symmetrical.

The profiles for 0.2% PAA LIV (Fig. 7(a)) also show a change from slight asymmetry to the left at $Re = 1870$ and 7695 to pronounced asymmetry to the right at $Re = 10{,}950$, whereas the intermediate profile ($Re = 3840$), for the early stage of transition, is essentially symmetrical. Due to its highly flexible molecular structure PAA is highly shear-thinning and viscoelastic and the much higher and extended range of Reynolds numbers for transitional flow is associated with the strongly drag-reducing character of this polymer (see e.g. [7]). The laminar flow profile at $Re = 1085$ and the turbulent flow profile at $Re = 18820$ are again symmetrical.

The first set of profiles from the CSIRO laboratory in Melbourne (Fig. 8(a)) is for 0.6% CMC, a shear-thinning, viscoelastic polymer. The laminar ($Re = 750$) and turbulent flow ($Re = 3570$) profiles are clearly symmetric, whereas the transitional profile ($Re = 2180$) is skewed significantly to the right. For this fluid the fluctuation data are more limited (i.e. Fig. 8(b)).

The second set of data for Carbopol (Fig. 9(a)) is from the LEMTA laboratory in Nancy and for a higher concentration (0.2% compared with 0.1%) than the data from the Liverpool laboratory shown in Fig. 6(a). For this concentration the fluid displays more of a yield-stress behaviour and the viscosity data, plotted in Fig. 2 as shear stress against shear rate to emphasise the yield-stress behaviour, are well represented by the Herschel–Bulkley model. The higher concentration produces much flatter velocity profiles, similar to those for Laponite (Fig. 4(a)) which also displayed a yield-stress, but the laminar flow profile at the lowest Reynolds number ($Re = 681$) is again symmetrical while the transitional profiles ($Re = 1196$–4794) show increasing asymmetry to the left, just as for the lower concentration. The profile for $Re = 5289$, which may still be transitional, and that for $Re = 8920$, which appears to be fully turbulent, have again become completely symmetrical.

The 0.08% Ultrez data from CSIRO (Fig. 10(a)) show much the same trends as the data for 0.2% Carbopol: the laminar flow profiles ($Re = 1370$ and 1530) are flat and

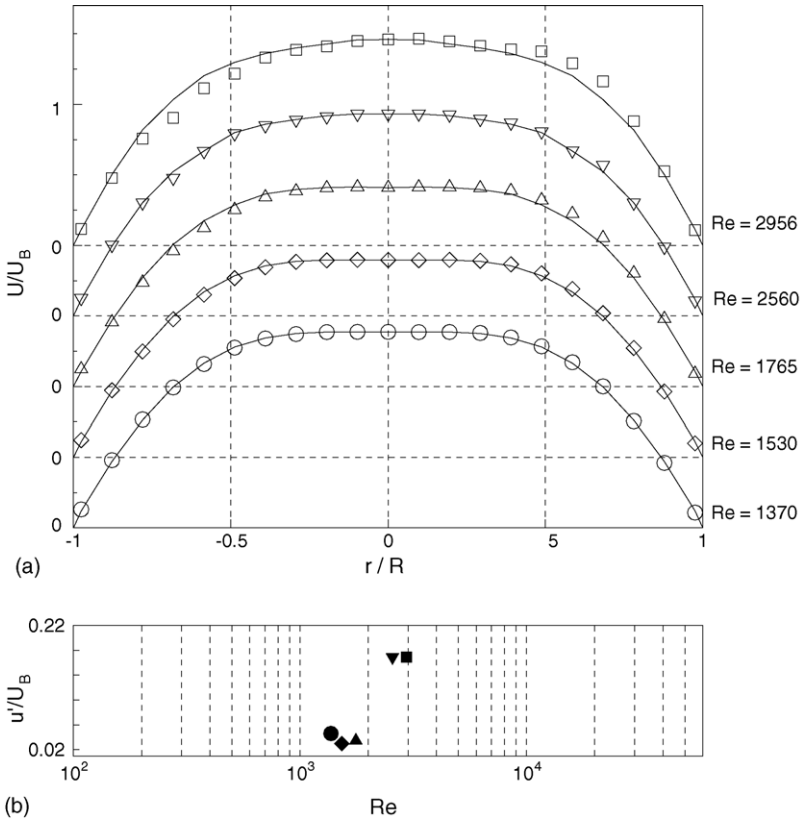

Fig. 10. (a) Mean axial velocity profiles for 0.08% ULTREZ CSIRO (including average data line) and (b) axial fluctuation level at $r/R = 0.8$ to indicate transition.

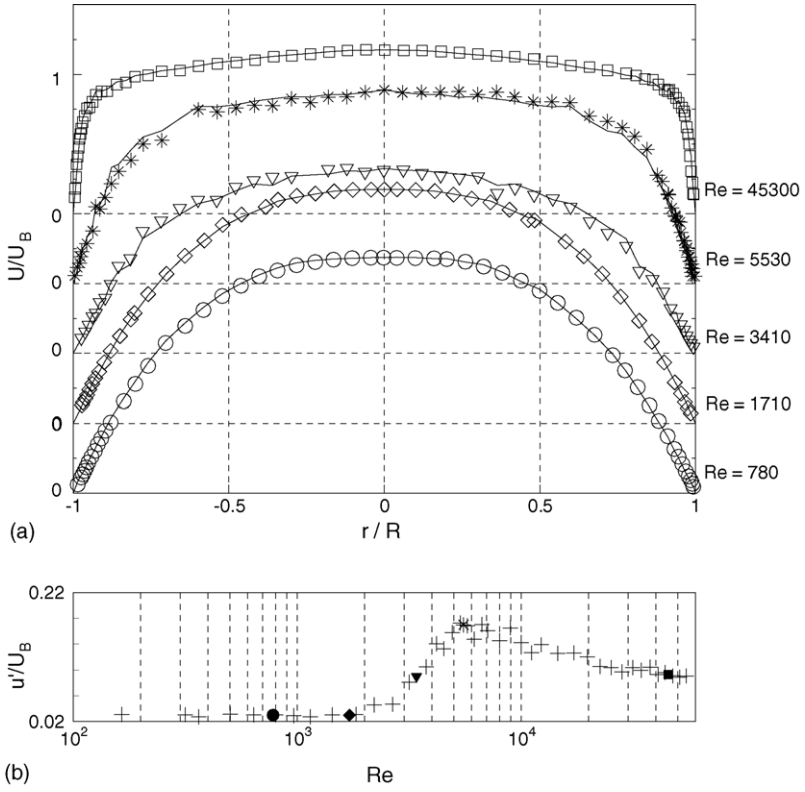

Fig. 11. (a) Mean axial velocity profiles for 0.09% CMC/0.09% XG LIV (including average data line) and (b) axial fluctuation level at $r/R = 0.8$ to indicate transition.

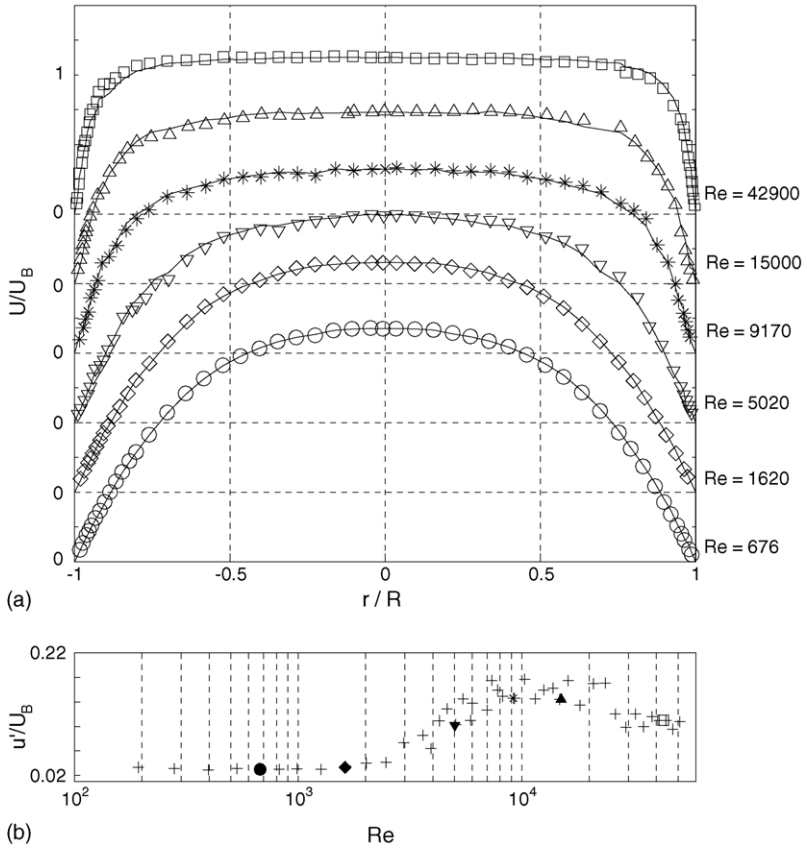

Fig. 12. (a) Mean axial velocity profiles for 0.125% PAA LIV (including average data line) and (b) axial fluctuation level at $r/R = 0.8$ to indicate transition.

symmetrical whereas the profiles at the start ($Re = 1765$) and end ($Re = 2956$) of transition are asymmetrical but to the right. The intermediate profile ($Re = 2560$), which is also close to the end of transition, however, is symmetrical.

The remaining velocity profiles, for 0.09% CMC/0.09% XG (Fig. 11(a)), 0.125% PAA (Fig. 12(a)) and 0.25% CMC (Fig. 13(a)) are all for shear-thinning viscoelastic polymer flows. Slight asymmetry is apparent for the CMC/XG blend at $Re = 5530$, at the end of transition, and for 0.125% PAA in the latter stages ($Re = 5020$ and 9170) of transition, but all other profiles are symmetrical within the measurement uncertainty.

5. Discussion and conclusions

The experimental velocity profile data, which we have presented, reveal to varying degrees departures from axisymmetry in fully developed pipe flow of a wide range of non-Newtonian liquids with rheological characteristics including shear-thinning viscosity, yield-stress and viscoelasticity. In all cases axisymmetry is maintained for laminar and turbulent flow conditions, and this is also the case for some transitional flows. For certain fluids, both yield-stress and viscoelastic (all are shear-thinning), asymmetry, to varying degrees, is apparent at all stages of transition from laminar to turbulent flow, i.e. from the first indications to almost fully developed turbulence. The data were obtained completely independently in laboratories in UK, France and Australia in quite different pipe flow facilities. The fact that symmetrical velocity profiles are obtained for both laminar and turbulent flow of all non-Newtonian fluids in all three laboratories leads us to the conclusion that the asymmetry must be a consequence of a fluid-dynamic mechanism rather than imperfections in the flow facilities. This conclusion is supported by the study of Eliahou et al. [5] on transition of pipe flow of a Newtonian fluid that found that asymmetric distortion of the mean velocity profiles required the imposition of a high-amplitude asymmetric disturbance. A more subtle indication that the asymmetry is fluid-dynamic in origin is the observation that the asymmetry can be of either sense and change sense as the Reynolds number changes, and this also suggests that the effect is not primarily due to the inherent Coriolis acceleration. In any event, for most of the flows under consideration here the Ekman numbers are too high (see Table 3) for Coriolis effects to play a role. It is also the case that the influences of buoyancy forces arising due to ambient temperature gradients or longitudinal curvature of the pipe runs are both too weak to induce asymmetry for the experimental conditions considered.

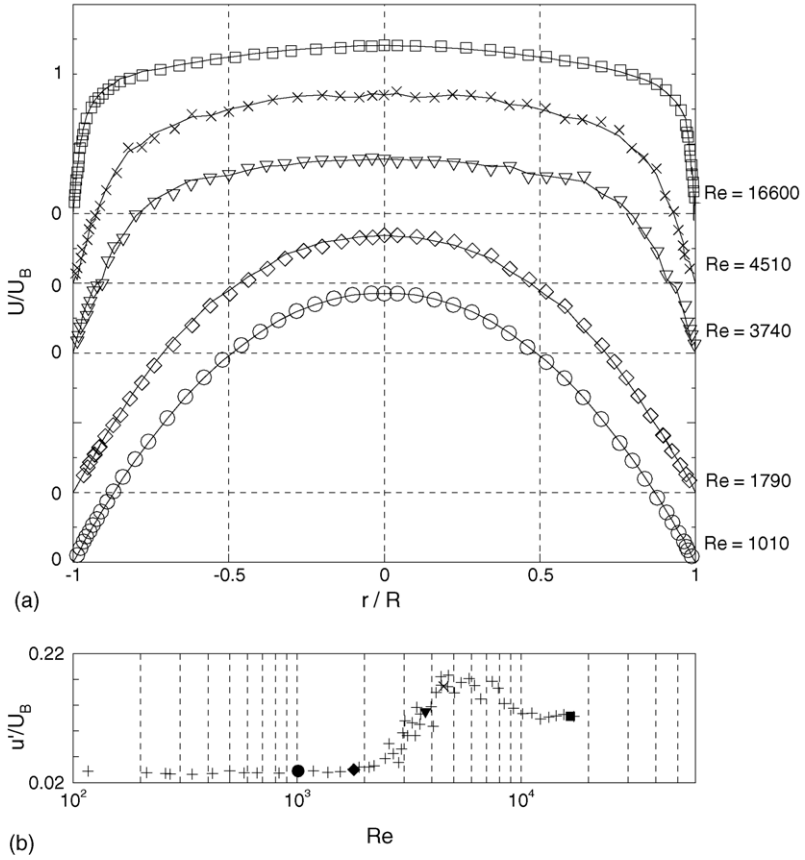

Fig. 13. (a) Mean axial velocity profiles for 0.25% CMC LIV (including average data line) and (b) axial fluctuation level at $r/R = 0.8$ to indicate transition.

Table 3
Fluid and flow parameters for all test fluids

Fluid	D (mm)	U_B (m/s)	ρ (kg/m^3)	$\dot{\gamma}_W$ (1/s)	μ_W (Pa s)	$Re = \frac{\rho U_B D}{\mu_W}$	$Ek = \frac{\mu_W}{2\Omega\rho D^2 \sin\alpha}$
Glycerine LIV	100	0.0398	1119	–	0.0082	540	5
		0.0733		–		1000	5
		0.160		–		2200	–
		0.178		–		2400	–
		0.258		–		3500	–
Water LIV	100	0.360	1000	–	0.001	36000	–
		0.610		–	0.001	61000	–
0.25% CMC LIV	100	0.580	1000	46	0.0573	1010	39
		0.899		72	0.0502	1790	35
		1.31		197	0.0351	3740	–
		1.45		246	0.0321	4510	–
		2.66		1244	0.0160	16600	–
0.09% CMC/0.09% XG LIV	100	0.300	1000	27	0.0384	780	26
		0.520		47	0.0304	1710	21
		0.917		62	0.0269	3410	–
		0.979		166	0.0177	5530	–
		3.13		1749	0.0069	45300	–
0.2% XG LIV	100	0.433	1000	59, 17	0.0267, 0.058	1620	18, 40
		0.923		167	0.0142	6500	–
		1.390		326	0.00988	14100	–
		2.52		895	0.00621	40500	–

Table 3 (*Continued*)

Fluid	D (mm)	U_B (m/s)	ρ (kg/m^3)	$\dot{\gamma}_W$ (1/s)	μ_W (Pa s)	$Re = \frac{\rho U_B D}{\mu_W}$	$Ek = \frac{\mu_W}{2\Omega\rho D^2 \sin\alpha}$
0.125% PAA LIV	100	0.256	1000	26	0.0379	676	26
		0.447		45	0.0276	1620	19
		0.939		94	0.0187	5020	–
		1.302		169	0.0142	9170	–
		1.670		315	0.0111	15000	–
		3.360		940	0.0078	42900	–
0.2% PAA LIV	100	0.564	1000	56	0.0520	1085	36
		0.791		79	0.0423	1870	29
		1.252		125	0.0326	3840	22
		1.754		246	0.0228	7695	–
		2.340		281, 518	0.0214, 0.0166	10950	–
		2.450		1080	0.0130	18820	–
0.1% CARB EZ1 LIV	100	0.328	1000	31	0.0489	670	34
		0.547,		57	0.0391	1400	27
		0.796		54	0.0398	2000	27
		1.05		84	0.0339	3100	23
		1.04		236	0.0235	5570	–
		1.78		479	0.0185	9600	–
		2.95		1660	0.0123	24000	–
1.5% LAP LIV	100	0.52	1000	72	0.0945	550	65
		0.84		113	0.0659	1275	45
		0.90		144	0.0545	1650	37
		1.06		244	0.0366	2900	25
		1.09		293	0.0321	3400	–
		2.03		2500	0.00802	25300	–
0.6% CMC CSIRO	105	1.22	1000	53	0.170	750	174
		3.18		73	0.153	2180	–
		4.35		124	0.128	3570	–
0.08% ULTREZ CSIRO	105	2.0	1000	262	0.146	1370	150
		2.2		267	0.144	1530	148
		2.4		293	0.136	1765	140
		2.97		371	0.116	2560	–
		3.34		386	0.113	2956	–
0.2% CARB LEMTA	30	2.25	1000	808	0.099	681	1026
		3.56		1273	0.089	1196	911
		6.13		2169	0.066	2780	675
		7.21		2478	0.054	3996	
		8.13		2788	0.051	4794	
		6.93		2329	0.039	5289	
		8.58		2829	0.029	8920	

The observations of asymmetry for transitional flow were not central to any of the experimental investigations reported here and a systematic study of transitional flow of yield-stress and other shear-thinning liquids is now underway in Liverpool and Nancy with emphasis on the issue of asymmetry. Throughout this paper we have referred to asymmetry in terms of left hand and right hand with respect to the pipe centreline. We are well aware that the measurements have been confined to horizontal traverses and that the three dimensionality of the mean-flow structures concerned is most unlikely to be symmetrical about the horizontal plane. Other aspects of the new study will be to investigate the full three dimensionality, including the possibility that the flows develop a helical structure along the pipe axis, why the asymmetry (or helicity) is fixed rather than precessing and why the orientation is repeatable for a given fluid and flow.

References

[1] J.J. Allan, C.A. Greated, W.D. McComb, Laser-Doppler anemometer measurements of turbulent structure in non-Newtonian fluids, J. Phys. D Appl. Phys. 17 (1984) 533.
[2] J.S. Chung, W.P. Graebel, Laser anemometer measurements of turbulence in non-Newtonian pipe flows, Phys. Fluids 15 (1972) 546.
[3] W.R. Dean, Note on the motion of a fluid in a curved pipe, Philos. Mag. 4 (1927) 208.
[4] A. Draad, F.T.M. Nieuwstadt, The Earth's rotation and laminar pipe flow, J. Fluid Mech. 361 (1998) 297.
[5] S. Eliahou, A. Tumin, I. Wygnanski, Laminar–turbulent transition in Poiseuille pipe flow subjected to periodic perturbation emanating from the wall, J. Fluid Mech. 361 (1998) 333.
[6] M.P. Escudier, F. Presti, Pipe flow of a thixotropic liquid, J. Non-Newt. Fluid Mech. 62 (1996) 291.
[7] M.P. Escudier, F. Presti, S. Smith, Drag reduction in the turbulent pipe flow of polymers, J. Non-Newt. Fluid Mech. 81 (1999) 197.

[8] L.J.W. Graham, L. Pullum, An investigation of complex hybrid suspension flows by magnetic resonance imaging, Can. J. Chem. Eng. 80 (2002) 200.
[9] W.D. McComb, L.H. Rabie, Part II: laser-Doppler measurements of turbulent structure, AIChE J. 28 (1982) 558.
[10] T. Mizushina, H. Usui, Reduction of eddy diffusion for momentum and heat in viscoelastic fluid flow in a circular pipe, Phys. Fluids 20 (1977) 100.
[11] A.S. Pereira, F.T. Pinho, Turbulent pipe flow characteristics of low molecular weight polymer solutions, J. Non-Newt. Fluid Mech. 55 (1994) 321.
[12] A.S. Pereira, F.T. Pinho, Turbulent pipe flow of thixotropic fluids, Int. J. Heat Fluid Flow 23 (2002) 36.
[13] J. Peixinho, C. Nouar, C. Desaubry B. Theron, Laminar transitional and turbulent flow of yield stress fluid in a pipe, in press.
[14] F.T. Pinho, J.H. Whitelaw, Flow of non-Newtonian fluids in a pipe, J. Non-Newt. Fluid Mech. 34 (1990) 129.
[15] R.J. Poole, M.P. Escudier, Turbulent flow of viscoelastic liquids through an asymmetric sudden expansion, J. Non-Newt. Fluid Mech. 117 (2004) 25.
[16] P.K. Ptasinski, F.T.M. Nieuwstadt, B.H.A.A. van den Brule, M.A. Hulsen, Experiments in turbulent pipe flow with polymer additives at maximum drag reduction, Flow Turbulence Combust. 66 (2001) 159.
[17] P. Schuemmer, W. Thielen, Structure of turbulence in viscoelastic fluids, Chem. Eng. Commun. 4 (1980) 593.
[18] J.M.J. den Toonder, M.A. Hulsen, G.D.C. Kuiken, F.T.M. Nieuwstadt, Drag reduction by polymer additives in a turbulent pipe flow: numerical and laboratory experiments, J. Fluid Mech. 337 (1997) 193.
[19] F.M. White, Viscous Fluid Flow, second ed., McGraw-Hill, 1991.
[20] K. Yasuda, R.C. Armstrong, R.E. Cohen, Shear flow properties of concentrated solutions of linear and star branched polystyrenes, Rheol. Acta 20 (1981) 163.